Title: Vegetative phase change in *Populus tremula x alba*.

Authors: Erica H. Lawrence[1*], Aaron R. Leichty[1,2], Erin E. Doody[1], Cathleen Ma[3], Steven H. Strauss[3] and R. Scott Poethig[1]

[1]Department of Biology, University of Pennsylvania, Philadelphia, Pennsylvania, 19104 USA
[2]Department of Plant Biology, University of California, Davis, California, 95616 USA
[3]Department of Forest Ecosystems and Society, Oregon State University, Corvallis, Oregon 97331
*Corresponding author: lawrence.erica.h@gmail.com

Key Words: Development, Juvenile-to-Adult Transition, miR156, *Populus* (Poplar), Vegetative Phase Change

Main Body Word Count: 4713

Introduction: 690
Materials and Methods: 1432
Results: 2674
Discussion: 1157

Number of figures: 8 (all printing in color)
Number of tables: 0
Supplemental files: 2

Summary

- Plants transition through juvenile and adult phases of vegetative development in a process known as vegetative phase change (VPC). In poplars (genus *Populus*) the differences between these stages are subtle, making it difficult to determine when this transition occurs. Previous studies of VPC in poplars have relied on plants propagated *in vitro,* leaving the natural progression of this process unknown.

- We examined developmental morphology of seed-grown and *in vitro* derived *Populus tremula x alba* (clone 717-1B4), and compared the phenotype of these, to transgenics with manipulated miR156 expression, the master regulator of VPC.

- In seed-grown plants, most traits changed from node-to-node during the first 3 months of development but remained constant after node 25. Many traits remained unchanged in clones over-expressing miR156, or were enhanced when miR156 was lowered, demonstrating their natural progression is regulated by the miR156/SPL pathway. The characteristic leaf fluttering of *Populus* is one of these miR156-regulated traits.

- Vegetative development in plants grown from culture mirrored that of seed-grown plants, allowing direct comparison between plants often used in research and those found in nature. These results provide a foundation for further research on the role of VPC in the ecology and evolution of this economically important genus.

Introduction

During ontogeny, plants transition through distinct phases, which is reflected in morphological variation in the organs produced across development. These developmental transitions include the visually obvious transition between vegetative and reproductive growth as well as the often more subtle change between juvenile and adult vegetative stages, known as vegetative phase change (Ashby, 1948; Brink, 1962; Doorenbos, 1965; Poethig, 2013). In species with abrupt changes in vegetative morphology—termed *heteroblastic*—the distinction between the juvenile and adult phases is unambiguous (Zotz *et al.*, 2011). For example, many species of *Acacia* transition from producing bipinnate compound leaves to producing a simple undivided leaf termed a phyllode (Walters & Bartholomew, 1984). Other examples include *Eucalyptus globulus*, which transitions from producing ovate, wax-covered leaves to producing lanceolate glaucous leaves (James & Bell, 2001) and *Ipomoea caerulea,* which transitions from producing monolobed to trilobed leaves (Ashby, 1948). Vegetative phase change is more difficult to identify in species that experience less drastic changes in leaf and shoot morphology. As a result, we know little about the duration of juvenile and adult phases in different taxa, or the relationship between this developmental transition and other aspects of plant life history, such as

61 plant responses to biotic and abiotic conditions. However, even in these so-called *homoblastic*
62 species (Goebel, 1900), organs produced early in shoot development differ from those produced
63 later in development in a variety of morphological, anatomical, and physiological traits (Feng *et*
64 *al.*, 2016). Identifying these traits and determining which are components of vegetative phase
65 change as opposed to those regulated by other factors, such as plant size or chronological age, is
66 an important problem in plant development.

67 In *Arabidopsis* and most other plants, the transition from the juvenile to the adult phase of
68 vegetative development is regulated by the closely related microRNAs, miR156 and miR157
69 (Poethig, 2013; He *et al.*, 2018). These miRNAs directly repress members of the Squamosa
70 Promoter Binding Protein-Like (*SPL*) family of transcription factors (Rhoades *et al.*, 2002;
71 Schwab *et al.*, 2005) which promote adult traits (Xu *et al.*, 2016). During the juvenile phase
72 miR156/157 levels are high, but as plants age their expression declines, allowing for the
73 increased expression of their *SPL* targets. This coordinated change in miR156 and *SPL* gene
74 expression leads to the onset of adult traits, with different traits typically appearing at slightly
75 different times in shoot development, depending on their sensitivity to the level of SPL proteins
76 (He *et al.*, 2018).

77 Vegetative phase change is likely to be of particular importance in long-lived perennial
78 species such as trees, because the ability of these species to survive to reproductive competence
79 requires that they cope with changing conditions over a long period of time. Poplars are of
80 considerable economic and ecological importance and have become popular model systems for
81 tree biology due to their ability to be propagated in culture and susceptibility to *Agrobacterium*-
82 mediated transformation (Taylor, 2002). Leaf and shoot phenotypes of plants derived from
83 culture and over-expressing miR156 have been described in clones of *Populus x canendensis*
84 (Wang *et al.*, 2011) and *P. tremula x alba* (Rubinelli *et al.*, 2013). However, the significance of
85 this information for vegetative phase change in *Populus* is still unknown because these studies
86 lacked the earliest developmental stages and fine-scale timeline needed to capture vegetative
87 phase change, and relied on gain-of-function transgenics. Here, we compare the vegetative
88 phenotype of seed-grown *Populus tremula x alba* with plants originating from explants in tissue
89 culture across multiple timepoints during vegetative development, and identify phase-specific
90 traits using both gain- and loss-of-function miR156 transgenics. We found that shoot
91 development in plants propagated *in vitro* closely resembles the development of seed-grown

92 plants, and that vegetative phase change occurs very early in both types of shoots. Most of the
93 traits we examined changed significantly across shoot development and were sensitive to the
94 level of miR156. One of these was leaf fluttering, a trait that has a significant effect on
95 photosynthetic efficiency (Roden & Pearcy, 1993b). Our results provide basic information about
96 the nature of vegetative phase change in *Populus tremula x alba* and demonstrate that shoots
97 regenerated *in vitro* can be used as models of primary shoot development in this species.
98

99 **Materials and Methods**

100 *Plant transformation*

101 Assembly of Ubi10:AthMIR156a and Ubi10:MIM156 constructs have previously been
102 described (Feng *et al.*, 2016). Additionally, a second MIM156 construct was designed with
103 Golden Gate Cloning (Engler *et al.*, 2014) and used for a later transformation after losing many
104 of the original lines to a chamber malfunction. Further details of construct assembly can be found
105 in Table S1.

106 Poplar line 717-1B4 was transformed using *Agrobacterium tumefaciences* (strain *AGL1*)
107 following the protocol described in Filichkin *et al.* (2006). Briefly, leaf and stem explants were
108 selected on callus-induction, shoot induction, shoot elongation and rooting media using BASTA.
109 A total of 30 Ubi10:AthMIR156a events and 25 Ubi10:MIM156 events were isolated. PCR was
110 used to first screen for transgene insertion using two primer sets, each utilizing a primer to the
111 *Arabidopsis* UBIQUITIN 10 promoter and either the *MIR156a* or MIM156 sequence (Table S2).
112 Of these, we screened 28 Ubi:AthMIR156a lines and 19 Ubi10:MIM156 lines for levels of
113 miR156 and miR157 (Fig. S**1A-B**). Based on levels of miR156, two lines for each construct type
114 were selected (or based on availability in the case of event GG.MIM156-22). For the
115 Ubi10:AthMIR156a and Ubi10:MIM156 constructs made with the pCambia 3300 backbone, the
116 Ubi10:AthMIR156a construct had a higher rate of producing transgenic shoots (percent of
117 explants forming shoots was 52% versus 33.9%). We did not track efficiency for the other
118 MIM156 construct.
119

120 *Plant material and growth conditions*

121 *Populus tremula x alba* line 717-1B4, two independent miR156 over-expressing
122 (miR156OX) lines, 40 and 78, and two independent MIM156 lines, 22 and 84, were obtained by

123 *in vitro* propagation and hardening on propagation media as described in Meilan and Ma (2006).
124 Plants were then transplanted to Fafard-2 growing mix (Sungro Horticulture, Massachusetts,
125 USA) in 0.3-L pots in the greenhouse at the University of Pennsylvania (39.9493°N, 75.1995°W,
126 22.38 m a.s.l.) and kept in plastic bags for increased humidity for 2 weeks. Plants were
127 transferred to 4.2-L pots with Fafard-52 growing mix 3 weeks later and fertilized with Osmocote
128 14-14-14 (The Scotts Company, Marysville, OH, USA), supplemented by weekly applications of
129 Peters 20-10-20 (ICL Fertilizers, Dublin, OH, USA). Plants were grown at a temperature ranging
130 from 22 and 27°C on a 16 hr photoperiod, with illumination provided by a combination of
131 natural light and 400-W metal halide lamps (P.L. Light Systems, Ontario, Canada) with daily
132 irradiances between 300 and 1,500 μmol m^{-2} s^{-1} measured at the top of the canopy across the day.
133 Planting of individuals was staggered across three months with the position of plants in the
134 greenhouse randomized and individuals rotated frequently.
135 *Populus tremula x alba* seeds were purchased from Sheffield's Seed Company (Locke,
136 NY), and were germinated on a layer of vermiculite on top of Fafard-2 growing mix in 0.64-L
137 pots in the greenhouse under conditions described above. Seedlings were transplanted one month
138 after germination into Fafard-52 growing mix in 1.76-L pots, fertilized with Osmocote 14-14-14.
139 They were transplanted to 4.2-L pots 3 months later. Planting of individuals was staggered across
140 five months and individuals were rotated within the greenhouse frequently.
141
142 *mRNA and smRNA abundance*
143 For initial screening of miR156 and miR157 abundance, and follow-up validation of
144 selected lines, shoot apices with leaf primordia less than 3 cm were used. For characterization of
145 temporal patterns of miR156/157 and *SPL* abundance in seed-grown and culture derived plants,
146 leaf primordia smaller than 1 cm were sampled and pooled with at least 3 leaves per replicate.
147 For all plants, node or leaf positions are counted from the base of the plant where the first leaf
148 produced is number 1. Primordia were collected across the plant's lifespan to obtain samples for
149 each of the measured leaf positions when they were at the same stage of development, frozen
150 with liquid N_2, and stored at -70°C until all samples were ready for RNA extraction. Total RNA
151 was isolated using the Spectrum™ Plant Total RNA Kit (Sigma-Aldrich), according to the
152 manufacturer's instructions. smRNA levels were measured by RT-qPCR, using primers specific
153 for mature sequences of miR156, miR157 and miR159 in combination with the stem-loop RT

154 primers described in Varkonyi-Gasic et al. (2007) (Table S2). miR159 was used as an
155 endogenous control (Leichty & Poethig, 2019) and validated across time points in seed-grown
156 and culture derived plants (Fig. **S2**). cDNA was synthesized using Invitrogen SuperScript III
157 following the methods of Varkonyi-Gasic et al. (2007). Platinum Taq (Invitrogen) was used with
158 the Roche universal hydrolysis probe #21, and a three-step amplification protocol. For measuring
159 mRNA abundance, total RNA was DNase digested (Qiagen) followed by cDNA synthesis using
160 Invitrogen SuperScript III using each manufacturer's protocol and a polyT primer. *PtaACT2* or
161 *PtaCDC2* was used as the endogenous control (Pettengill *et al.*, 2012). Resulting cDNA was
162 quantified by qPCR using SYBR-Green Master Mix (Bimake) and primers specific to the
163 endogenous control and *SPL* genes (Table S2) with a three-step amplification protocol. Relative
164 measures of abundance were calculated using the $2^{-\Delta\Delta Ct}$ method (Livak & Schmittgen, 2001).
165
166 *Stomatal impressions, epidermal traits, petiole morphology and abaxial trichome density.*
167 Stomatal density and epidermal cell size were measured using clear nail polish
168 impressions of adaxial and abaxial surfaces of fully expanded leaves. Trichomes were removed
169 from the abaxial side of leaves with tape when necessary, and three sections per leaf were
170 imaged and photographed using an Olympus BX51 light microscope. Hand sections of leaf
171 petioles within 1 cm of leaf attachment site were imaged as described above. Trichome density
172 on the abaxial side of the leaf was measured using an Olympus MVX10 dissecting scope.
173 Measurements were made along the mid vein, where the density was low enough to permit
174 accurate counts. All measurements and counts were made using Fiji software (Schindelin *et al.*,
175 2012).
176
177 *Leaf vein densities*
178 Sections from new fully expanded leaves were cleared using NaOH and bleach, and then
179 stained with Safranin following the protocol described in Scoffoni and Sack (2013). Vein lengths
180 of all visible vein orders were measured from microscope images using Fiji software (Schindelin
181 *et al.*, 2012), and vein densities were calculated following Scoffoni and Sack (2013).
182
183 *Leaf shape and size*

184 Fully expanded leaves were attached to paper using double-sided tape, labeled by node
185 number increasing from the base of the plant, and scanned. The scanned images were measured
186 using the Morphological Analysis of Size and Shape (MASS) software (Chuanromanee *et al.*,
187 2019). The SHAPE program (Iwata & Ukai, 2002) and Fiji (Schindelin *et al.*, 2012) was used to
188 determine the number of serrations and the perimeter of the leaf. The perimeter of the leaf was
189 measured from the tops of the serrations so as not to include the added length from the serration
190 indentations. Serrations were analyzed relative to the leaf perimeter so that the data were not
191 influenced by differences in overall leaf size.
192
193 *Leaf initiation rate, internode distance and branching*
194 The leaf initiation rate was determined by counting the node of the uppermost visible leaf
195 at least twice a week between 10 and 160 days of growth in seed-grown plants and between 32
196 and 55 days after transplant to soil in 717-1B4 lines. The number of branches at least 1 cm in
197 length between nodes 1 and 25 was determined after 4 months of growth in soil.
198
199 *Fluttering*
200 To measure leaf fluttering, plants were placed 100 cm away from a fan, with the leaf to
201 be measured facing perpendicular to the wind. Wind speeds at the sample leaf position were 1.5
202 m/s as measured with an anemometer. Leaf movement was filmed at 240 fps for 30 seconds
203 (representative example in supplemental file "Poplar Fluttering Video"). Leaf movement was
204 analyzed by following the movement of a mark placed at the tip of the leaf using Tracker video
205 analysis and modeling tool v5.0.7. The height and width of the petiole were measured using a
206 digital caliper.
207
208 *Statistical Analysis*
209 All statistical analyses were performed in JMP® Pro v. 14.0.0 (SAS Institute Inc., Cary,
210 NC). Traits in seed-grown poplar across leaf positions were measured from a minimum of 42
211 individuals and fit with a linear or second-degree polynomial as appropriate with p-values and R^2
212 values reported. Traits that were examined at multiple leaf positions in 717 wildtype, MIM156
213 lines 84 and 22 and miR156OX lines 40 and 78 were measured from a minimum of 6 individuals
214 and compared by ANCOVA and a Student's t test ($\alpha = 0.05$) where leaf position and genotype

were the main effects. Whole-plant measures of branching and internode length in these plants was compared by one-way ANOVA where genotype was the main effect and a Student's *t* test ($\alpha = 0.05$), and leaf emergence was compared by ANCOVA with days after transplant and genotype as the main effects.

Results

Isolation of MIR156a over-expressing and MIM156 plants

For the lines with confirmed transgene insertions, the relative abundance of miR156 averaged 0.63 and 1.37 for the MIM156 and *MIR156a* lines, respectively (Figure **S1A,B**). Lines MIR156A-78 and MIR156-40 were selected as strong and moderate miR156 over-expressors, respectively (Figure **S1A**). Line MIM156-84 was selected as a strong miR156 mimic, while line MIM156-22 was selected to represent a transgenic line in which the miR156 level was not significantly different from wildtype (Figure **S1A,B**, *T*-test: $p = 0.51$). The levels of miR156-targeted *SPL* genes was consistent with the levels of miR156/157 in different transgenic lines. MIM156-84 had, respectively, 3- and 9-fold more *PtSPL24* and *PtSPL23* transcripts relative to wildtype (Figure **S1C**). As expected based on its levels of miR156, the transcripts of both *PtSPL24* and *PtSPL23* in MIM156-22 did not differ from wildtype (Figure **S1C**). Both MIR156A-40 and MIR156A-78 showed significantly lower levels of these same genes when compared with wildtype (Figure **S1C**). To confirm the specificity of these transgenes, we also measured levels of *PtSPL4* and *PtSPL7*—genes with no predicted miR156 target site. In both cases, there was no clear pattern of transcript abundance across transgenic lines (Figure **S1C**).

miR156/157 and ptSPL24 abundance in seed-grown plants and 717-1B4 lines

Patterns of miR156/157 abundance in the leaf primordia of seed-grown plants matched that previously reported for other species, such as *A. thaliana* and *Vachellia* sp. (He *et al.*, 2018; Leichty & Poethig, 2019). miR156/157 abundance dropped 7-fold between nodes 1 and 10, followed by a slower decline in successive nodes (Fig. **1A**). We first determined that the control small RNA, miR159, was present at the same level in leaves 15 and 25 of seed-grown plants and the clone 717-1B4 (Fig. **S2**), and then used this transcript to normalize the level of miR156/157 in wild-type and transgenic genotypes of 717-1B4. The abundance of miR156/157 in the primordia of leaf 15 and 25 in wildtype 717-1B4 was similar to the amount of miR156/157 in

246 these same leaves in seed-grown poplar (Fig. **1A, B**), suggesting that miR156/157 are expressed
247 at comparable levels at the same node in plants propagated by these methods. Leaf 15 and 25 of
248 the miR156OX lines had, respectively 4.9 and 5.6 times the amount of miR156 as wild-type
249 leaves, a level comparable to that of leaf 3 and 5 of seed-grown plants (Fig. **1A, B**). Although the
250 amount of miR156/157 in leaves 15 and 25 of the MIM156 lines was similar to that in 717-1B4
251 and seed-grown poplar (Fig. **1A, B**), line 84 had approximately 1/3 the amount of miR156 at an
252 earlier stage of development, before it was transferred to soil (Fig. **S1A**). Target mimics do not
253 necessarily reduce the level of their target miRNAs (Franco-Zorrilla *et al.*, 2007), so the
254 significance of these MIM156 data is difficult to interpret. In any case, the similarity between the
255 amount of miR156/157 in MIM156 and wild-type lines shows that the transformation protocol
256 and vector components have no independent effect on miR156/157 abundance.
257 To determine if the changes in miR156/157 abundance observed in seed- and culture-
258 derived plants were large enough to have downstream effects on the expression of their *SPL*
259 targets, we measured *ptSPL24* abundance across nodes 1 and 34 in seed-grown plants and at
260 nodes 15 and 25 of 717-1B4 lines. *ptSPL24* abundance increased more than 11-fold between
261 nodes 1 and 34 in seed-grown plants (Fig. **2A**). In wildtype 717-1B4, *ptSPL24* abundance
262 increased 2-fold between nodes 15 and 25 (Fig. **2B**). Across a similar span in seed-grown plants,
263 *ptSPL24* abundance increased by more than 1.5-fold between nodes 12 and 22, again indicating
264 that the expression patterns of genes in the miR156/157-SPL pathway are comparable between
265 similar nodes of plants propagated via seeds and cuttings. Leaves 15 and 25 in the miR156OX
266 lines had 4- and 15-fold less *ptSPL24* respectively, compared to these same nodes in the wildtype
267 line. This is consistent with the levels of miR156/157 in these lines, and indicates that these
268 levels of miR156/157 are functionally significant. The abundance of *ptSPL24* in MIM156 line 22
269 was similar to wild-type, consistent with the observation that the abundance of miR156 in this
270 line is not significantly different from wildtype. Interestingly, the abundance of *ptSPL24* was
271 more than 2-fold greater in leaf 15 of MIM156 line 84 compared to wildtype, although the level
272 of miR156/157 in this transgenic leaf is similar to wildtype. There was no difference in the
273 abundance of *ptSPL24* at node 25 in MIM156 line 8 and wildtype plants . Together with the
274 abundance of miR156 and *ptSPL24* measured in young plants still in culture (Fig. **S1**), these data
275 suggest that the MIM156 transgene has the greatest effect during the juvenile phase, when
276 miR156 levels are naturally high.

277

278 *Changes in miR156 abundance alter plant growth rate and form*

279 Plants grown from seed produced leaves at a relatively slow rate for the first few weeks
280 after planting, and transitioned to a faster, linear growth rate after producing 15-20 leaves (Fig.
281 **3A**). Leaf initiation in wild-type and transgenic clones of 717-1B4 was delayed for 35-40 days
282 after transplanting to soil, and then occurred at increasing rate over the next 2-3 weeks of
283 measurement. During this latter period, miR156OX lines had higher rates of leaf initiation than
284 either wild-type or MIM156 lines (Fig. **3B**). miR156OX lines also had shorter internodes than
285 either the wild-type and MIM156 lines (Fig. **3C**) and produced significantly more axillary
286 branches after 3 months than these genotypes (Fig. **3D**, Photographs of plants at this age in Fig.
287 **S3**). The MIM156 lines were not significantly different from 717-1B4 for any of these traits,
288 although these lines did have slightly longer internodes than 717-1B4.

289

290 *Juvenile and adult leaves differ in leaf shape and size*

291 The leaves of seed-grown plants became gradually rounder (decreased L:W ratio) (Fig.
292 **4A**) and larger (Fig. **4C**) from node 1 to node 25 and did not change significantly in shape or size
293 after this point (Fig. **4C, 1C**). 717-1B4 displayed a similar trend, although the leaves of this
294 clone reached their climax shape and size a few nodes earlier than seed-grown plants (Fig. **4B, D**
295 and **5**). MIM156 lines did not differ significantly in size from 717-1B4, but the leaves of line 84
296 were rounder than 717-1B4 beginning at node 15. In contrast, the leaves of miR156OX lines
297 were significantly more elongated and smaller than wild-type leaves starting from node 15
298 (Student's *t* test $p < 0.05$). These results suggest that changes in leaf shape and size during shoot
299 development in poplar are partly regulated by a decrease in level of miR156.

300 To obtain a comprehensive picture of the effect of miR156 on leaf morphology in
301 *Populus tremula x alba*, we also measured the specific leaf area, serrations, stomatal density,
302 epidermal cell area, abaxial trichome density, and petiole morphology of successive leaves. We
303 examined every 5th leaf of seed-grown plants from germination to node 45-50, and every 5th
304 leaf of 717-1B4 and transgenic lines from node 10 to 25. We observed greater variation for these
305 traits in seed-grown plants compared to the culture-derived clones likely because of the increased
306 genetic variation in these open-pollinated plants.

307 Specific leaf area (SLA) is the area of the leaf blade per unit mass, and is determined by
308 the thickness of the leaf blade and cell density. SLA impacts leaf physiology through changes in
309 intra-leaf light dynamics, CO_2 diffusion and the distribution of leaf N (Parkhurst, 1994; Epron *et*
310 *al.*, 1995; Terashima & Hikosaka, 1995; Reich *et al.*, 1998; Terashima *et al.*, 2006; Evans *et al.*,
311 2009), and therefore provides insights into how changes in leaf development alter function. SLA
312 decreased in a curvilinear fashion from leaf 5 to leaf 40 in seed-grown plants and decreased
313 linearly from leaf 10 to leaf 25 in 717-1B4 and the 4 transgenic lines (Figure **4E, F**). However,
314 SLA decreased nearly linearly between leaf 10 and leaf 25 in seed-grown plants, so these data do
315 not reveal if there is a significant difference in the pattern in seed-grown and clonally propagated
316 plants. On the other hand, we found that—at nodes 15-25—lines over-expressing miR156 had a
317 significantly higher SLA, and one MIM156 line (84) had a significantly lower SLA, than 717-
318 1B4 at node 10 (Student's *t* test, $p < 0.05$ and $p < 0.0001$ for miR156OX lines at nodes 15 and 20,
319 and node 25 respectively and $p = 0.019$ for line 84 node 10). These results suggest that SLA is a
320 phase-specific trait and is regulated by miR156.
321 Leaf serrations are present on leaves of all measured positions for both seed- and culture-
322 derived plants. To account for significant differences in leaf size, serration numbers are
323 normalized to leaf perimeter. We found there to be a slight decrease in the number of serrations
324 per cm of leaf perimeter in seed-grown plants, decreasing from just over 2 at node 10 to around
325 1.5 at node 35 (Fig. **4G**). 717-1B4 lines showed no phase-specific differences in the number of
326 serrations ($p = 0.1469$) as leaves of all genotypes and all positions had between 0.64 and 0.97
327 serrations per cm leaf perimeter (Fig. **4H**). It is unclear as to why culture-derived plants have
328 lower serration density than seed-grown plants however, these small differences in serrations are
329 not likely to have any biological significance.
330 Stomatal density on both the adaxial and abaxial side of the leaf changed across leaf
331 positions, but in opposite directions (Fig. **4I, K**). In seed-grown plants, adaxial stomatal density
332 decreased linearly from leaf 5 to leaf 40, whereas abaxial stomatal density increased linearly
333 over this interval; at every node, the density of stomata on the adaxial surface of the leaf was
334 significantly less than that on the abaxial surface. Both 717-1B4 and the MIM156 lines had a
335 very low density of adaxial stomata on leaf 10, and this number was reduced to nearly zero on
336 leaf 25. In contrast, the density of abaxial stomata in these genotypes increased significantly
337 between leaf 10 and leaf 25. In the miR156OX lines, the density of stomata on both the adaxial

338 and abaxial surfaces of leaves 10 and 25 was essentially identical to that of the basal-most leaves
339 of seed-grown plants. Thus, miR156 has a role in regulating stomatal density on both sides of the
340 leaf. However, other factors are also likely to contribute to the developmental changes in
341 stomatal density (Berger & Altmann, 2000; Sugano *et al.*, 2010), because this parameter changes
342 linearly during shoot development, rather than in the curvilinear pattern characteristic of the
343 change in miR156 levels (Fig. **4J, L**).
344 We measured epidermal cell area by taking impressions of the adaxial epidermis, because
345 the high density of trichomes made it impractical to measure this trait on the abaxial surface. In
346 seed-grown plants, cell area decreased approximately 4-fold over the first 30 leaves and
347 remained relatively constant after this point (Fig. **4M**). In 717-1B4, cell area decreased about 2-
348 fold from leaf 10 to leaf 20, and decreased much less dramatically, if at all, between leaf 20 and
349 leaf 25. The MIM156 lines were not significantly different from 717-1B4. In contrast, cell area
350 in the miR156OX did not change significantly between leaf 10 and leaf 25 (Fig. **4N**). These
351 results suggest that epidermal cell area is a phase-specific trait.
352 The leaves of *Populus alba* appear white because of a dense layer of trichomes on the
353 abaxial surface of the leaf blade, and this trait is also characteristic of *P. tremula x alba* (Fig **S3**).
354 All the leaves of *P. tremula x alba* produced abaxial trichomes, but trichome density increased
355 dramatically during shoot growth (Fig. **4O, P**). In seed-grown plants, abaxial trichome density
356 increased more than 10-fold between leaf 5 and leaf 40 and increased by about 6-fold between
357 leaf 10 and leaf 25 in 717-1B4. In contrast, abaxial trichome density remained at the same
358 relatively low level from node 10 to node 25 in the miR156OX, and it increased significantly
359 more than 717-1B4 in both MIM156 lines (Student's *t* test; $p < 0.01$ and $p < 0.0001$ for line 22 and
360 84 respectively). This result suggests that abaxial trichome production is a phase-specific trait in
361 *P. tremula x alba* and is hypersensitive to the level of miR156.
362
363 *Leaf vein density increases as plants transition from juvenile to adult*
364 While working with the 717-1B4 lines, we noticed differences in vasculature of leaves at
365 the same position between wildtype and transgenic lines. Because vein density and patterning
366 impacts leaf structure and function (i.e. assimilation and herbivore resistance) (Brodribb *et al.*,
367 2007; Blonder *et al.*, 2018), we thought this trait was worth investigating. Leaf vein density
368 increased 1.8-fold with increasing leaf position in 717-1B4 and in the MIM156 lines, although

369 MIM156 line 84 had a significantly higher vein density than 717-1B4 in leaf 10 (Student's *t* test,
370 $p < 0.01$). Similar results were obtained for the density of vein endings. In the miR156OX lines,
371 vein density and the density of vein endings did not differ much between leaf 10 and leaf 25, and
372 were identical to, or slightly lower than, the values observed for leaf 10 in 717-1B4 (Fig. **6**).
373
374 *Petiole morphology changes during development leading to altered leaf fluttering behavior*
375 Many species of poplar, including *Populus tremula x alba,* exhibit leaf fluttering, a trait
376 that has been attributed to the vertical elongation of the petiole (Niklas, 1991). In a previous
377 study of *Populus x canadensis*, we found that the petioles of *in vitro* propagated plants became
378 increasing elongated as the shoot developed, and that over-expression of miR156 suppressed this
379 process (Wang et al. 2011). To determine if this phenomenon occurs naturally, we examined the
380 L:W ratio of a cross-section of the petiole in seed-grown *Populus tremula x alba* (Fig. **7A, D**).
381 We found that the petiole of leaves at node 10 was slightly broader than tall (L:W < 1), whereas
382 the petioles of leaves at higher nodes became vertically elongated (L:W >1), reaching their
383 climax shape around node 40. In wild-type 717-1B4, and in the MIM156 and miR156OX lines,
384 the petiole also became progressively elongated (Fig. **7B, C**). However, the miR156OX lines had
385 significantly less elongated petioles than the 717-1B4 and the MIM156 lines, and reached a
386 maximum L:W ratio at an earlier node. We also examined the effect of these transgenes on
387 petiole anatomy. In 717-1B4, the petioles of leaves at nodes 10 and 15 had an adaxial
388 indentation, a large central vascular bundle, and two smaller vascular bundles located in a
389 horizontal plane above the central bundle. The petioles of leaves 20 and 25 lacked an adaxial
390 indentation and had three vertically oriented vascular bundles that decreased in size from the
391 abaxial to the adaxial side of the petiole. In the MIM156 lines, the vascular anatomy of leaf 15
392 was intermediate between that of leaf 10 and leaf 20 in 717-1B4, indicating that the transition to
393 the adult shape is accelerated in these lines, despite the lack of a significant change in the L:W
394 ratio of the petiole (Fig. **7C**). Consistent with their L:W ratio, lines over-expressing miR156
395 retained a juvenile petiole morphology up to at least node 25. Petiole anatomy is therefore an
396 obvious qualitative indicator of the phase identity of a leaf in *Populus tremula x alba*.
397 To determine if this change in petiole morphology has an effect on the behavior of the
398 leaf, we looked at two measures of leaf fluttering—the total distance moved by the leaf, and the
399 maximum horizontal span of the leaf tip—when leaves were exposed to a constant wind velocity

400 (Fig. **8A, S4**). There was a statistically significant (p <0.0001) positive linear relationship
401 between petiole L:W ratio and these fluttering measures in 717-1B4, the MIM156 and
402 miR156OX lines. Leaves at basal node 10 in the 717-1B4 and in the MIM156 lines fluttered less
403 than leaves at more apical node 25, whereas juvenile leaves at node 25 of the miR156OX lines
404 fluttered less than leaves at node 25 of the 717-1B4 and in the MIM156 lines (Fig. **8B, C**). Thus,
405 the petiole morphology of juvenile and adult leaves of *Populus tremula x alba* has a significant
406 effect on their response to wind.
407
408 **Discussion**
409 Many plants lack visually abrupt changes in form during shoot development, making the
410 onset of vegetative phase change difficult to observe. As a result, the existence of this
411 phenomenon and its significance for plant ecology and evolution are often under appreciated. In
412 this study, we characterized the growth rate, developmental morphology, and temporal pattern of
413 miR156 and *SPL* expression in *Populus tremula x alba,* an ecologically and economically
414 important tree. We found that many leaf traits change during shoot development in plants grown
415 from seeds, as well as in shoots arising *de novo* in culture, and that most of these changes are
416 correlated with and sensitive to changes in the level of miR156. These data confirm and extend
417 previous studies of the effect of miR156 on *Populus* development (Wang *et al.*, 2011; Rubinelli
418 *et al.*, 2013), and provide a foundation for future research on the function of vegetative phase
419 change in the life history of this woody species.
420 In nature, poplars propagate primarily from adventitious shoots, whereas clones used for
421 research or commercial purposes are propagated from axillary buds or by inducing shoot
422 regeneration *in vitro* (Taylor, 2002). The extent to which these plants recapitulate the
423 development of the primary shoot is still unknown. We found by at least the 10th node, the
424 development of a regenerated shoot is remarkably similar to that of a seed-grown plants. This
425 result suggests that the phase-identity of poplar cells is either re-set during the de-differentiation
426 of the primary tissue sample, or during shoot regeneration, and is consistent with observations in
427 *Zea mays* (Irish & Karlen, 1998; Orkwiszewski & Poethig, 2000). This observation also raises
428 the long-standing question of whether differentiated traits can be maintained in tissue culture.
429 Although vegetative phase change sometimes involves traits unique to a particular
430 species (Wang *et al.*, 2011; Leichty & Poethig, 2019), analyses of plants with altered levels of

431 miR156 have revealed a number of phase-specific traits that are common to phylogenetically
432 diverse species. In *Zea mays*, *Arabidopsis thaliana*, *Nicotiana tabacum,* and now *Populus*
433 *tremula x alba*, these traits include patterns of trichome production, leaf shape and size,
434 epidermal and stomatal cell traits, vein density, leaf initiation rate, and branching (Bongard-
435 Pierce *et al.*, 1996; Telfer *et al.*, 1997; Feng *et al.*, 2016; He *et al.*, 2018). At least some of these
436 traits are also regulated by miR156 in *Populus x canadensis* (Wang *et al.*, 2011), rice (Xie *et al.*,
437 2006), alfalfa (Aung *et al.*, 2015), switchgrass (Fu *et al.*, 2012), *Lotus japonicus* (Wang, 2014),
438 and tomato (Zhang *et al.*, 2011). This observation indicates that vegetative phase change is an
439 ancient and fundamental aspect of shoot development, and also suggests that the differential
440 expression of various traits during shoot development contributes to plant fitness and is therefore
441 under natural selection (Leichty & Poethig, 2019).
442 Determining how phase-specific traits contribute to plant fitness is challenging. However,
443 a number of studies have shown that plants over-expressing miR156 are more or less sensitive to
444 various environmental stresses (Stief *et al.*, 2014; Cui *et al.*, 2014; Arshad *et al.*, 2017; Kang *et*
445 *al.*, 2020), Despite this, there is still little evidence that juvenile and adult phases of wild type
446 plants display these same differences in sensitivity or how they might contribute to plant fitness.
447 There are relatively few examples of phase-specific vegetative traits that are either known or
448 expected to be selectively advantageous (Williams *et al.*, 1998; Holeski *et al.*, 2009; Leichty &
449 Poethig, 2019). Our observation that adult leaves flutter more than juvenile leaves is another
450 such example. In poplar, leaf fluttering is beneficial under high-light and high-heat
451 environments, but is disadvantageous under low light conditions as it reduces photosynthesis
452 (Roden & Pearcy, 1993a,b). This suggests that reduced leaf fluttering is advantageous early in
453 development, when plants are more likely to be shaded, whereas increased fluttering is
454 advantageous once plants are no longer in the understory.
455 Surprisingly, we found that progression of vegetative phase change in poplar, a woody
456 perennial, is not very different from this process *Arabidopsis*, an annual herb. In *P. tremula x*
457 *alba,* the onset of adult traits begins within three months of growth, despite the much longer
458 lifespan of this species. As in *Arabidopsis* (He *et al.*, 2018), miR156 expression in poplar
459 declines rapidly over the first few leaves, but it isn't until later, when the decline in miR156 is
460 more subtle, that adult morphological traits first appear. This result further supports the findings
461 in *Arabidopsis* that miR156/157 expression in early leaves far exceeds the amount necessary to

462 repress most *SPL* targets (He *et al.*, 2018). Further, these finding suggest that it is inappropriate
463 to assume the timing of vegetative phase change is proportional to the lifespan of a species. As
464 we continue to characterize this developmental transition across species with diverse life
465 histories, we are likely to find large variations in the proportion of time spent in either the
466 juvenile or adult vegetative phase.

467 During shoot development, different morphological and physiological traits change in a
468 coordinated fashion, but not necessarily at the same node or at the same rate (Hackett & Murray,
469 1997; Leichty & Poethig, 2019). Furthermore, under certain conditions, traits can become
470 dissociated, resulting in leaves or shoots that have unusual combinations of juvenile and adult
471 traits (Robbins, 1960; Doorenbos, 1965). In our experiments, this was apparent from the
472 phenotype of transgenic lines expressing a miR156/miR157 target site mimic (MIM156). The
473 stronger of these transgenes had a significant effect on leaf L:W ratio, SLA, epidermal cell area,
474 petiole morphology and leaf vein density, but did not affect leaf initiation rate, stomatal density
475 and petiole L:W ratio. These observations are consistent with studies in *Arabidopsis*, which show
476 that different miR156-regulated *SPL* genes have different transcription patterns and sensitivity to
477 miR156 abundance (Xu *et al.*, 2016; He *et al.*, 2018). Along with the evidence that *SPL* genes
478 also have different loss-of-function phenotypes (Xu *et al.*, 2016), these results suggest that
479 variability in the expression of different phase-specific traits may arise from the differential
480 response of functionally distinct *SPL* genes to changes in the level of miR156.

481 miR156 and its *SPL* targets control many economically important traits, including
482 flowering time, shoot architecture, biomass and lignin production, pest and disease resistance
483 and abiotic stress responses (Wang & Wang, 2015). In the biofuel crop *P. virgatum*, for example,
484 over-expressing miR156 leads to increases in biomass, digestibility, and lignin production, a
485 delay in flowering time, and altered susceptibility to the pathogen *Puccinia emaculata* (Chuck *et*
486 *al.*, 2011; Fu *et al.*, 2012; Baxter *et al.*, 2018). Similar effects of miR156 over-expression have
487 been observed in the forage legumes *Trifolium pretense* (Zheng *et al.*, 2016) and *Medicago*
488 *sativa* (Aung *et al.*, 2015). Poplars are fast-growing trees useful for a wide variety of industrial
489 purposes, as well for the re-forestation of degraded land (Taylor, 2002). The ability to engineer
490 their chemistry and vegetative development through the manipulation of miR156 offers new
491 opportunities for the improvement of this important group of plants.
492

Acknowledgements

We thank Samara Gray and Joshua Darfler for their assistance in caring for the plants used in this study. This research was funded by the NSF Graduate Research Fellowship (DGE-1845298), U. of Pennsylvania SAS Dissertation Research Fellowship and the Peachey Research Fund to E.H.L., NIH T32GM008216 to A.R.L and NIH GM51893 to R.S.P.

Author Contributions

E.H.L., A.R.L., and R.S.P. planned and designed the research. E.H.L. and A.R.L. performed the experiments. C.M., and S.H.S. helped create the transgenics used in this study. E.E.D performed follow-up experiments during revision. E.H.L performed statistical analyses and wrote the first draft of the manuscript. All authors revised and provided comments on the manuscript.

References

Arshad M, Feyissa BA, Amyot L, Aung B, Hannoufa A. **2017**. MicroRNA156 improves drought stress tolerance in alfalfa (Medicago sativa) by silencing SPL13. *Plant Science* **258**: 122–136.

Ashby E. **1948**. Studies in the morphogenesis of leaves. II. The area, cell size and cell number of leaves of Ipomoea in relation to their position on the shoot. *New Phytologist* **47**: 177–195.

Aung B, Gruber MY, Amyot L, Omari K, Bertrand A, Hannoufa A. **2015**. Ectopic expression of LjmiR156 delays flowering, enhances shoot branching, and improves forage quality in alfalfa. *Plant Biotechnology Reports* **9**: 379–393.

Baxter HL, Mazarei M, Dumitrache A, Natzke JM, Rodriguez M, Gou J, Fu C, Sykes RW, Turner GB, Davis MF, *et al.* 2018. Transgenic miR156 switchgrass in the field: growth, recalcitrance and rust susceptibility. *Plant Biotechnology Journal* **16**: 39–49.

Berger D, Altmann T. **2000**. A subtilisin-like serine protease involved in the regulation of stomatal density and distribution in Arabidopsis thaliana. *Genes and Development* **14**: 1119–1131.

Blonder B, Salinas N, Patrick Bentley L, Shenkin A, Porroa POC, Tejeira YV, Espinoza TEB, Goldsmith GR, Enrico L, Martin R, *et al.* 2018. Structural and defensive roles of angiosperm leaf venation network reticulation across an Andes–Amazon elevation gradient. *Journal of Ecology* **106**: 1683–1699.

524 **Bongard-Pierce DK, Evans MMS, Poethig RS**. **1996**. Heteroblastic features of leaf anatomy in
525 maize and their genetic regulation. *International Journal of Plant Sciences* **157**: 331.
526 **Brink RA**. **1962**. Phase change in higher plants and somatic cell heredity. *The Quarterly Review*
527 *of Biology* **37**: 1–22.
528 **Brodribb TJ, Feild TS, Jordan GJ**. **2007**. Leaf maximum photosynthetic rate and venation are
529 linked by hydraulics. *Plant Physiology* **144**: 1890–1898.
530 **Chuanromanee TS, Cohen JI, Ryan GL**. **2019**. Morphological Analysis of Size and Shape
531 (MASS): An integrative software program for morphometric analyses of leaves. *Applications in*
532 *Plant Sciences* **7**: e11288.
533 **Chuck GS, Tobias C, Sun L, Kraemer F, Li C, Dibble D, Arora R, Bragg JN, Vogel JP,**
534 **Singh S, *et al.* 2011**. Overexpression of the maize Corngrass1 microRNA prevents flowering,
535 improves digestibility, and increases starch content of switchgrass. *Proceedings of the National*
536 *Academy of Sciences* **109**: 995–995.
537 **Cui L-G, Shan J-X, Shi M, Gao J-P, Lin H-X**. **2014**. The miR156-SPL9-DFR pathway
538 coordinates the relationship between development and abiotic stress tolerance in plants. *The*
539 *Plant Journal* **80**: 1108–1117.
540 **Doorenbos J**. **1965**. Juvenile and adult phases in woody plants. *Encyl. Plant Physiol.* **15**: 1222–
541 35.
542 **Engler C, Youles M, Gruetzner R, Ehnert T-M, Werner S, Jones JDG, Patron NJ,**
543 **Marillonnet S**. **2014**. A Golden Gate modular cloning toolbox for plants. *ACS Synthetic Biology*
544 **3**: 839–843.
545 **Epron D, Godard D, Cornic G, Genty B**. **1995**. Limitation of net CO2 assimilation rate by
546 internal resistances to CO2 transfer in the leaves of two tree species (Fagus sylvatica L. and
547 Castanea sativa Mill.). *Plant, Cell & Environment* **18**: 43–51.
548 **Evans JR, Kaldenhoff R, Genty B, Terashima I**. **2009**. Resistances along the CO2 diffusion
549 pathway inside leaves. *Journal of Experimental Botany* **60**: 2235–2248.
550 **Feng S, Xu Y, Guo C, Zheng J, Zhou B, Zhang Y, Ding Y, Zhang L, Zhu Z, Wang H, *et al.***
551 **2016**. Modulation of miR156 to identify traits associated with vegetative phase change in
552 tobacco (Nicotiana tabacum). *Journal of Experimental Botany* **67**: 1493–1504.
553 **Filichkin SA, Meilan R, Busov VB, Ma C, Brunner AM, Strauss SH**. **2006**. Alcohol-
554 inducible gene expression in transgenic Populus. *Plant Cell Reports* **25**: 660–667.

555 **Franco-Zorrilla JM, Valli A, Todesco M, Mateos I, Puga MI, Rubio-Somoza I, Leyva A,**
556 **Weigel D, García JA, Paz-Ares J, *et al.* 2007**. Target mimicry provides a new mechanism for
557 regulation of microRNA activity. *Nature Genetics* **39**: 1033–1037.
558 **Fu C, Sunkar R, Zhou C, Shen H, Zhang J-YY, Matts J, Wolf J, Mann DGJ, Stewart CN,**
559 **Tang Y, *et al.* 2012**. Overexpression of miR156 in switchgrass (Panicum virgatum L.) results in
560 various morphological alterations and leads to improved biomass production. *Plant*
561 *Biotechnology Journal* **10**: 443–452.
562 **Goebel K**. **1900**. *Organography of Plants Part I. General Organography. (English Translation*
563 *by I. B. Balfour)*. Oxford: Clarendon Press.
564 **Hackett WP, Murray JR**. **1997**. Approaches to understanding maturation or phase change. In:
565 Geneve RL, Preece JE, Merkle SA, eds. Biotechnology of Ornamental Plants. New York: CAB
566 International, 73–86.
567 **He J, Xu M, Willmann MR, McCormick K, Hu T, Yang L, Starker CG, Voytas DF, Meyers**
568 **BC, Poethig RS**. **2018**. Threshold-dependent repression of SPL gene expression by
569 miR156/miR157 controls vegetative phase change in Arabidopsis thaliana. *PLOS Genetics* **14**:
570 e1007337.
571 **Holeski LM, Kearsley MJC, Whitham TG**. **2009**. Separating ontogenetic and environmental
572 determination of resistance to herbivory in cottonwood. *Ecology* **90**: 2969–2973.
573 **Irish EE, Karlen S**. **1998**. Restoration of juvenility in maize shoots by meristem culture.
574 *International Journal of Plant Sciences* **159**: 695–701.
575 **Iwata H, Ukai Y**. **2002**. SHAPE: a computer program package for quantitative evaluation of
576 biological shapes based on elliptic Fourier descriptors. *The Journal of heredity* **93**: 384–385.
577 **James SA, Bell DT**. **2001**. Leaf morphological and anatomical characteristics of heteroblastic
578 Eucalyptus globulus ssp. Globulus (Myrtaceae). *Australian Journal of Botany* **49**: 259–269.
579 **Kang T, Yu CY, Liu Y, Song WM, Bao Y, Guo XT, Li B, Zhang HX**. **2020**. Subtly
580 manipulated expression of ZmmiR156 in tobacco improves drought and salt tolerance without
581 changing the architecture of transgenic plants. *Frontiers in Plant Science* **10**: 1664.
582 **Leichty AR, Poethig RS**. **2019**. Development and evolution of age-dependent defenses in ant-
583 acacias. *Proceedings of the National Academy of Sciences* **116**: 15596–15601.
584 **Livak KJ, Schmittgen TD**. **2001**. Analysis of relative gene expression data using real-time
585 quantitative PCR and the 2-ΔΔCT method. *Methods* **25**: 402–408.

586 **Meilan R, Ma C**. **2006**. Poplar (Populus spp.). In: Wang K, ed. Methods in Molecular Biology:
587 Agrobacterium Protocols. Totowa, NJ: Humana Press Inc., 143–151.
588 **Niklas KJ**. **1991**. The elastic moduli and mechanics of Populus tremuloides (Salicaceae) petioles
589 in bending. *American Journal of Botany* **78**: 989–996.
590 **Orkwiszewski JAJ, Poethig RS**. **2000**. Phase identity of the maize leaf is determined after leaf
591 initiation. *PNAS* **97**: 10631–10636.
592 **Parkhurst DF**. **1994**. Diffusion of CO2 and other gases inside leaves. *New Phytologist* **126**:
593 449–479.
594 **Pettengill EA, Parmentier-Line C, Coleman GD**. **2012**. Evaluation of qPCR reference genes in
595 two genotypes of Populus for use in photoperiod and low-temperature studies. *BMC Research*
596 *Notes* **5**.
597 **Poethig RS**. **2013**. Vegetative phase change and shoot maturation in plants. *Current Topics in*
598 *Developmental Biology* **105**: 125–152.
599 **Reich PB, Ellsworth DS, Walters MB**. **1998**. Leaf structure (specific leaf area) modulates
600 photosynthesis–nitrogen relations: evidence from within and across species and functional
601 groups. *Functional Ecology* **12**: 948–958.
602 **Rhoades MW, Reinhart BJ, Lim LP, Burge CB, Bartel B, Bartel DP**. **2002**. Prediction of
603 plant microRNA targets. *Cell* **110**: 513–520.
604 **Robbins WJ**. **1960**. Further observations on juvenile and adult Hedera. *American Journal of*
605 *Botany* **47**: 485–491.
606 **Roden JS, Pearcy RW**. **1993a**. Effect of leaf flutter on the light environment of poplars.
607 *Oecologia* **93**: 201–207.
608 **Roden JS, Pearcy RW**. **1993b**. The effect of flutter on the temperature of poplar leaves and its
609 implications for carbon gain. *Plant, Cell and Environment* **16**: 571–577.
610 **Rubinelli PM, Chuck G, Li X, Meilan R**. **2013**. Constitutive expression of the Corngrass1
611 microRNA in poplar affects plant architecture and stem lignin content and composition. *Biomass*
612 *and Bioenergy* **54**: 312–321.
613 **Schindelin J, Arganda-Carreras I, Frise E, Kaynig V, Longair M, Pietzsch T, Preibisch S,**
614 **Rueden C, Saalfeld S, Schmid B, *et al.* 2012**. Fiji: An open-source platform for biological-
615 image analysis. *Nature Methods* **9**: 676–682.
616 **Schwab R, Palatnik JF, Riester M, Schommer C, Schmid M, Weigel D**. **2005**. Specific

617 effects of microRNAs on the plant transcriptome. *Developmental Cell* **8**: 517–527.
618 **Scoffoni C, Sack L**. **2013**. Quantifying leaf vein traits. *Prometheus Wiki*.
619 **Stief A, Altmann S, Hoffmann K, Pant BD, Scheible W-R, Bäurle I**. **2014**. Arabidopsis
620 miR156 regulates tolerance to recurring environmental stress through SPL transcription factors.
621 *The Plant Cell* **26**: 1792–1807.
622 **Sugano SS, Shimada T, Imai Y, Okawa K, Tamai A, Mori M, Hara-Nishimura I**. **2010**.
623 Stomagen positively regulates stomatal density in Arabidopsis. *Nature* **463**: 241–244.
624 **Taylor G**. **2002**. Populus: Arabidopsis for forestry. Do we need a model tree? *Annals of Botany*
625 **90**: 681–689.
626 **Telfer A, Bollman KM, Poethig RS**. **1997**. Phase change and the regulation of trichome
627 distribution in Arabidopsis thaliana. *Development* **124**: 645–654.
628 **Terashima I, Hanba YT, Tazoe Y, Vyas P, Yano S**. **2006**. Irradiance and phenotype:
629 Comparative eco-development of sun and shade leaves in relation to photosynthetic CO2
630 diffusion. In: Journal of Experimental Botany. 343–354.
631 **Terashima I, Hikosaka K**. **1995**. Comparative ecophysiology of leaf and canopy
632 photosynthesis. *Plant, Cell & Environment* **18**: 1111–1128.
633 **Varkonyi-Gasic E, Wu R, Wood M, Walton EF, Hellens RP**. **2007**. Protocol: A highly
634 sensitive RT-PCR method for detection and quantification of microRNAs. *Plant Methods* **3**: 12.
635 **Walters GA, Bartholomew DP**. **1984**. Acacia Koa leaves and phyllodes: Gas exchange,
636 morphological, anatomical, and biochemical characteristics. *Botanical Gazette* **145**: 351–357.
637 **Wang J-W**. **2014**. Regulation of flowering time by the miR156-mediated age pathway. *Journal*
638 *of Experimental Botany* **65**: 4723–4730.
639 **Wang JW, Park MY, Wang LJ, Koo Y, Chen XY, Weigel D, Poethig RS**. **2011**. MiRNA
640 control of vegetative phase change in trees. *PLoS Genetics* **7**: e1002012.
641 **Wang H, Wang H**. **2015**. The miR156/SPL module, a regulatory hub and versatile toolbox,
642 gears up crops for enhanced agronomic traits. *Molecular Plant* **8**: 677–688.
643 **Williams WP, Davis FM, Buckley PM, Hedin PA, Baker GT, Luthe DS**. **1998**. Factors
644 associated with resistance to fall Armyworm (Lepidoptera: Noctuidae) and southwestern Corn
645 Borer (Lepidoptera: Crambidae) in corn at different vegetative stages. *Journal of Economic*
646 *Entomology* **91**: 1471–1480.
647 **Xie K, Wu C, Xiong L**. **2006**. Genomic organization, differential expression, and interaction of

648 SQUAMOSA Promoter-Binding-Like Transcription Factors and microRNA156 in Rice. *Plant*
649 *Physiology* **142**: 280–293.
650 **Xu M, Hu T, Zhao J, Park M-Y, Earley KW, Wu G, Yang L, Poethig RS**. **2016**.
651 Developmental functions of miR156-regulated SQUAMOSA PROMOTER BINDING
652 PROTEIN-LIKE (SPL) genes in arabidopsis thaliana. *PLOS Genetics* **12**: e1006263.
653 **Zhang X, Zou Z, Zhang J, Zhang Y, Han Q, Hu T, Xu X, Liu H, Li H, Ye Z**. **2011**. Over-
654 expression of sly-miR156a in tomato results in multiple vegetative and reproductive trait
655 alterations and partial phenocopy of the *sft* mutant. *FEBS Letters* **585**: 435–439.
656 **Zheng Q-L, Liu J, Goff BM, Dinkins RD, Zhu H**. **2016**. Genetic manipulation of miR156 for
657 improvement of biomass production and forage quality in Red Clover. *Crop Science* **56**.
658 **Zotz G, Wilhelm K, Becker A**. **2011**. Heteroblasty-a review. *Botanical Review* **77**: 109–151.
659
660

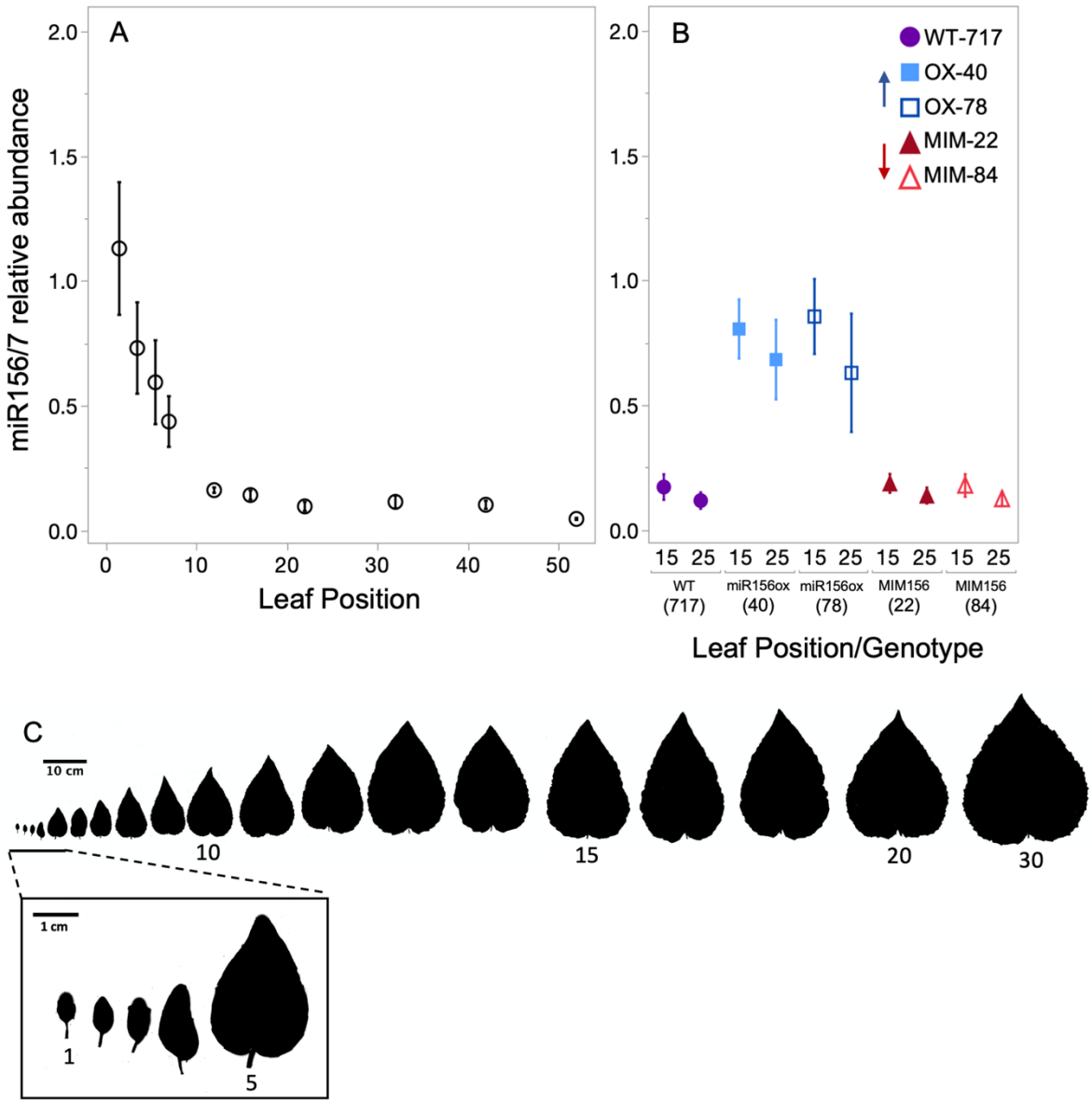

Figure 1. The relative abundance of miR156/157 in *Populus tremula x alba* leaf primordia grown from seed (A) or in transgenic and wildtype plants of the 717-1B4 clone initially propagated in tissue culture (B). All miR156/157 measurements are relative to the average of 4 replicates from seed-grown leaves 1 & 2. Data are presented as means ± s.e.m (n = 3) with seed-grown data depicted as black open circles, 717 wildtype by purple circles, miR156a overexpression lines depicted by blue squares and MIM156 lines depicted by red triangles. (C) Scans of successive leaves from nodes 1-17, 20 and 30 from plants grown from seed.

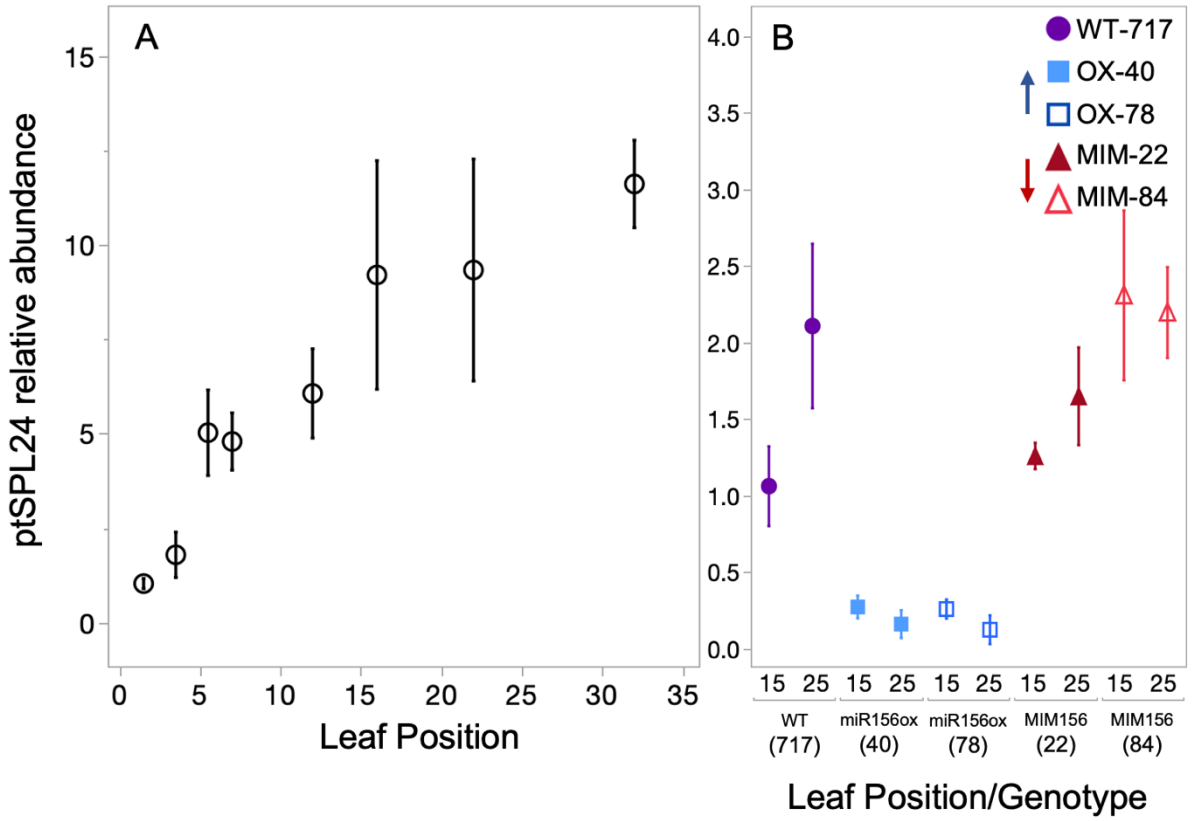

Figure 2. The relative abundance of *ptSPL24* transcripts in *Populus tremula x alba* leaf primordia grown from seed (A) or in transgenic and wildtype plants of the 717-1B4 background initially propagated in tissue culture (B). The abundance of *ptSPL24* in seed-grown plants relative to seed-grown leaves 1 & 2 (A) or relative to the abundance in wildtype 717 leaf 15 in plants initially propagated in tissue culture (B). Data presented as means ± s.e.m (n = 3) with see- grown data depicted as black open circles, 717 wildtype by purple circles, miR156a overexpression lines depicted by blue squares and MIM156 lines depicted by red triangles.

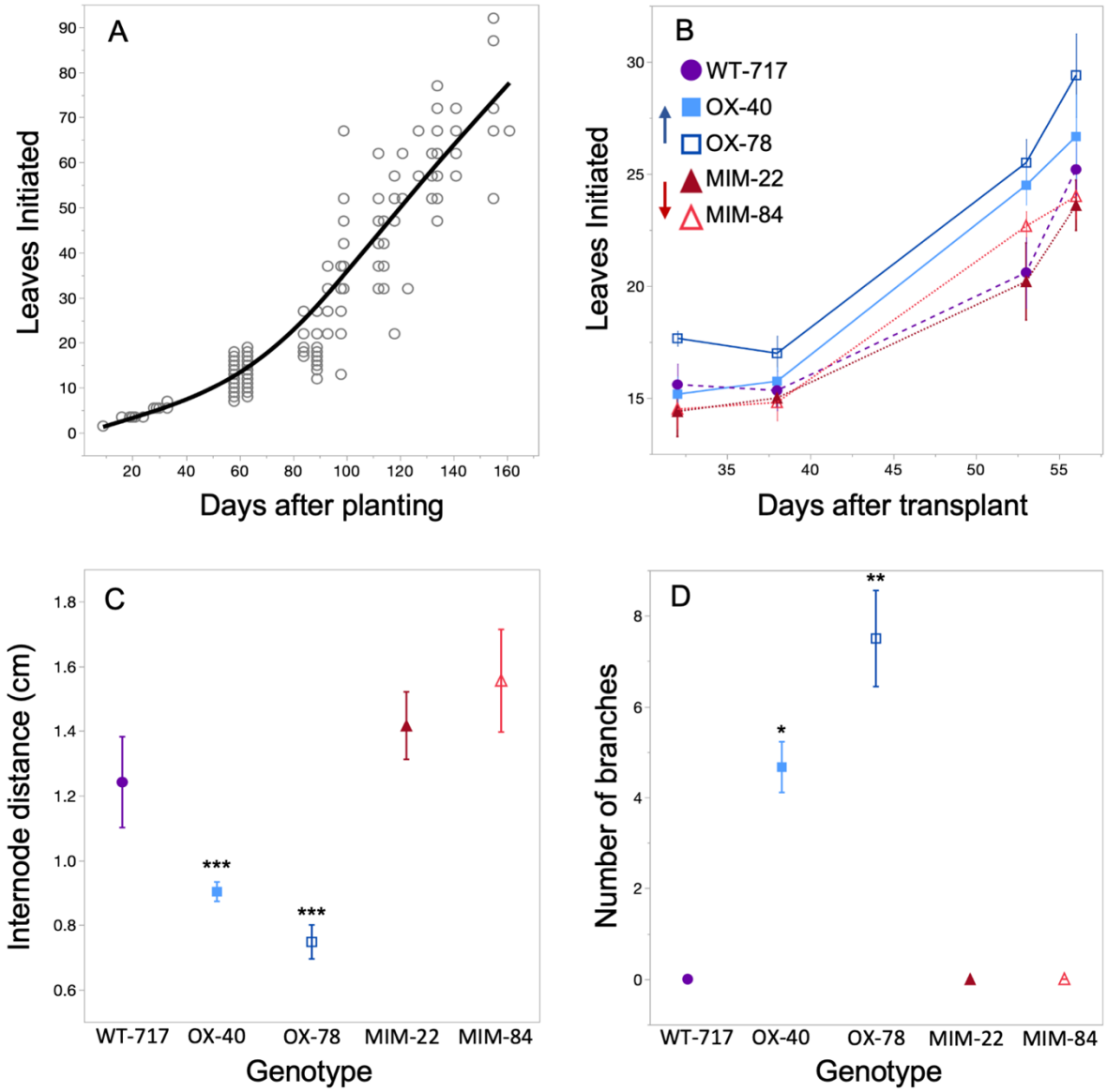

Figure 3. Number of leaves initiated by *P. tremula x alba* grown from seed (A) and the 717-1B4 wildtype and four transgenic lines initially propagated in tissue culture (n = 3-6) (B). The distance between nodes 10-20 (n = 6) (C), and the number of branches > 1cm in length between nodes 1 and 25 after 4 months of growth (n = 6) (D) in 717-1B4 and four transgenic lines. Data from seed-grown plants presented as individual biological replicates using grey open circles and a mean best fit line in black or as means ± s.e.m with 717 wildtype data depicted by purple circles, miR156*a* overexpression lines depicted by blue squares and MIM156 lines depicted by red triangles. Data in panel A show a second-degree polynomial fit with $p < 0.0001$ and R^2=0.92 and an ANCOVA for panel B found $p < 0.0001$ for genotype and days after transplant but no significance for an interaction between effects. One-way ANOVA for panels C and D found $p < 0.0001$ with the results of a *Student's t* between WT and mutants represented by * $p < 0.05$, ** $p < 0.01$, and *** $p < 0.001$.

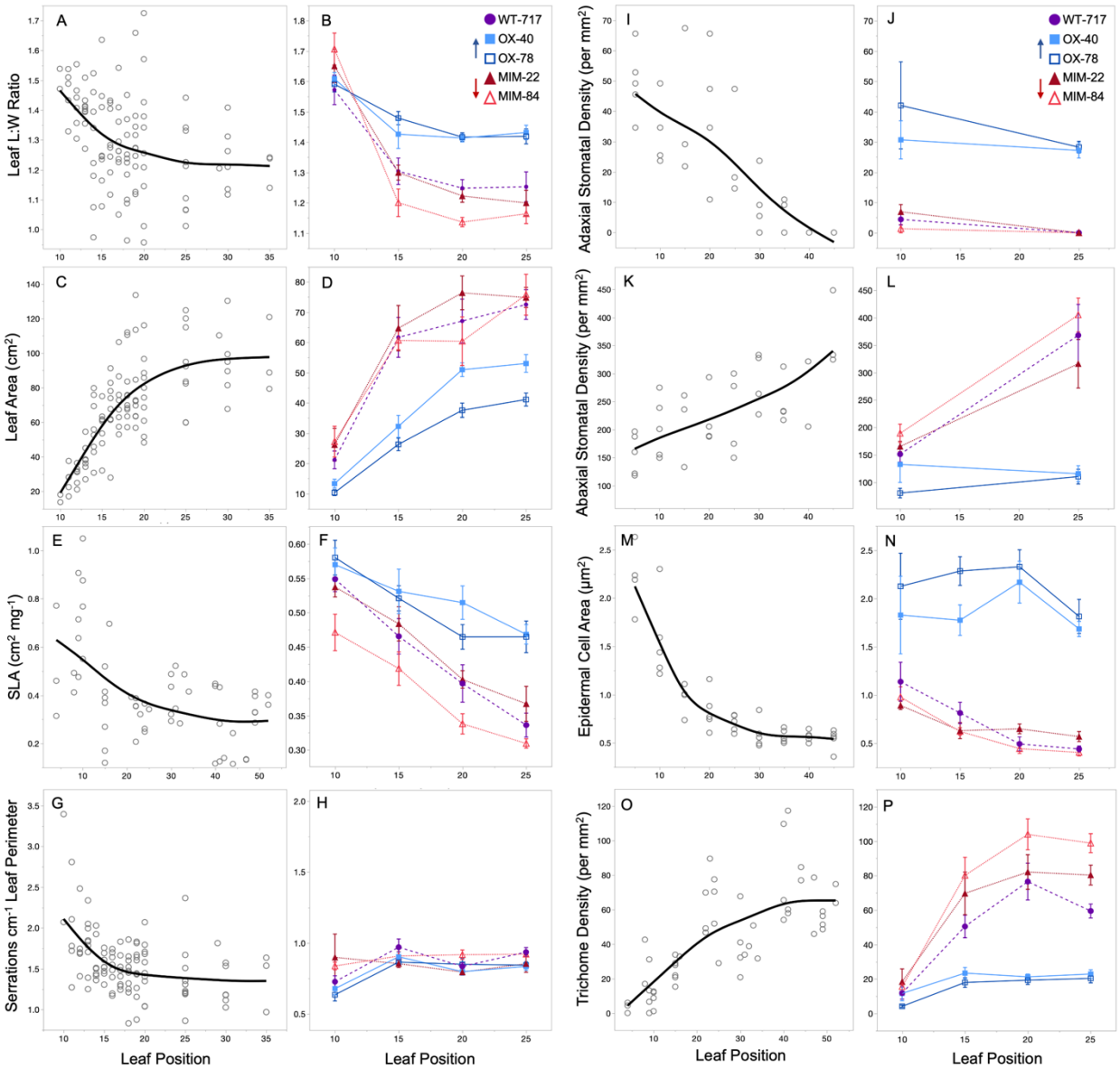

Figure 4. Leaf length:width (L:W) ratio, leaf area, specific leaf area (SLA), serrations per cm of leaf perimeter, adaxial stomatal density, abaxial stomatal density, adaxial epidermal cell area, and abaxial trichome density of seed-grown poplar (A, C, E, G, I, K, M, O) and the 717-1B4 and transgenic lines (B, D, F, H, J, L, N, P). Data from seed-grown plants presented as individual biological replicates using grey open circles and a mean best fit line in black or as means ± s.e.m with 717 wildtype data depicted by purple circles, miR156a overexpression lines depicted by blue squares and MIM156 lines depicted by red triangles (n = 5-11). Data in panels A, C, E, G, M and O show a second-degree polynomial relationship with p <0.0001 and R^2 values of 0.17, 0.6, 0.32, 0.25, 0.85 and 0.56 respectively. Data in panels I and K show a linear relationship with p <0.0001 and R^2 values of 0.58 and 0.46 respectively. ANCOVAs with leaf position and genotype as the effects for data in panels B, D, F, L, N and P found p <0.001 for both leaf position and genotype. In panel J, p <0.001 for genotype but N.S. for leaf position. In panel H, p < 0.01 for leaf position but N.S. for genotype. For the interaction between genotype and leaf position, p <0.05 for data in panels B, F, L, and P and N.S. for panels D, H, J, and N.

Figure 5. Representative plants from the wild-type 717-1B4, miR156a overexpressor line 40 and MIM156 line 84 two months following transplant from tissue culture. Leaves at positions 15 and 20 noted. Representative leaf shape for fully-expanded leaves from positions 10, 15, 20 and 25 in the 717-1B4 and transgenic poplar plants from tissue culture.

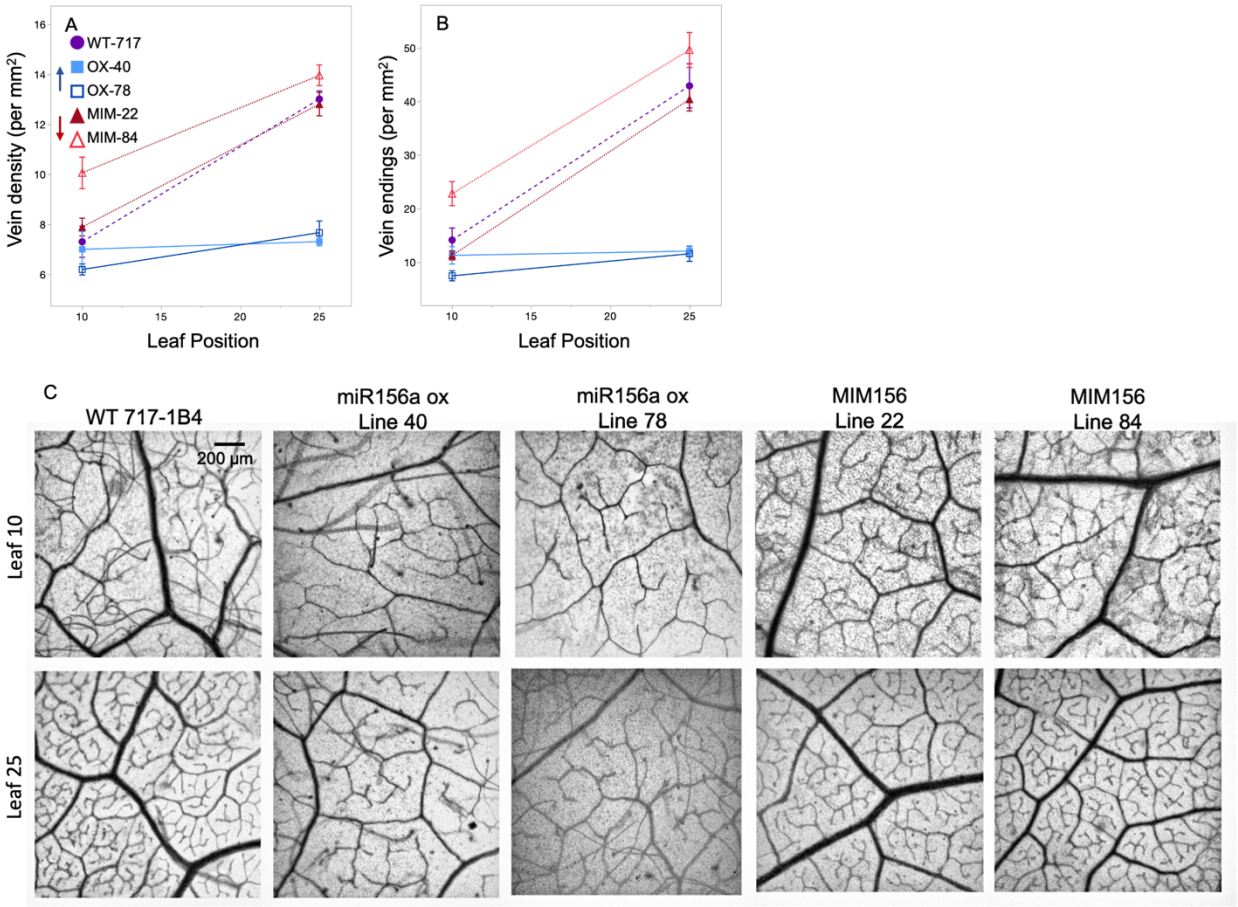

Figure 6. Total leaf vein density (A) and the number of vein endings (B) in the 717-1B4 and transgenic plants. Data from seed-grown plants presented as individual biological replicates using grey open circles and a mean best fit line in black or as means ± s.e.m with 717 wildtype data depicted by purple circles, miR156a overexpression lines depicted by blue squares and MIM156 lines depicted by red triangles (n = 5-6). ANCOVA with leaf position and genotype as the effects found p <0.0001 for both effects and the interaction for data in panels A and B. Representative samples of leaves cleared and stained to visualized vein density and architecture in leaves 10 and 25 of 717-1B4 and transgenic poplar lines (C).

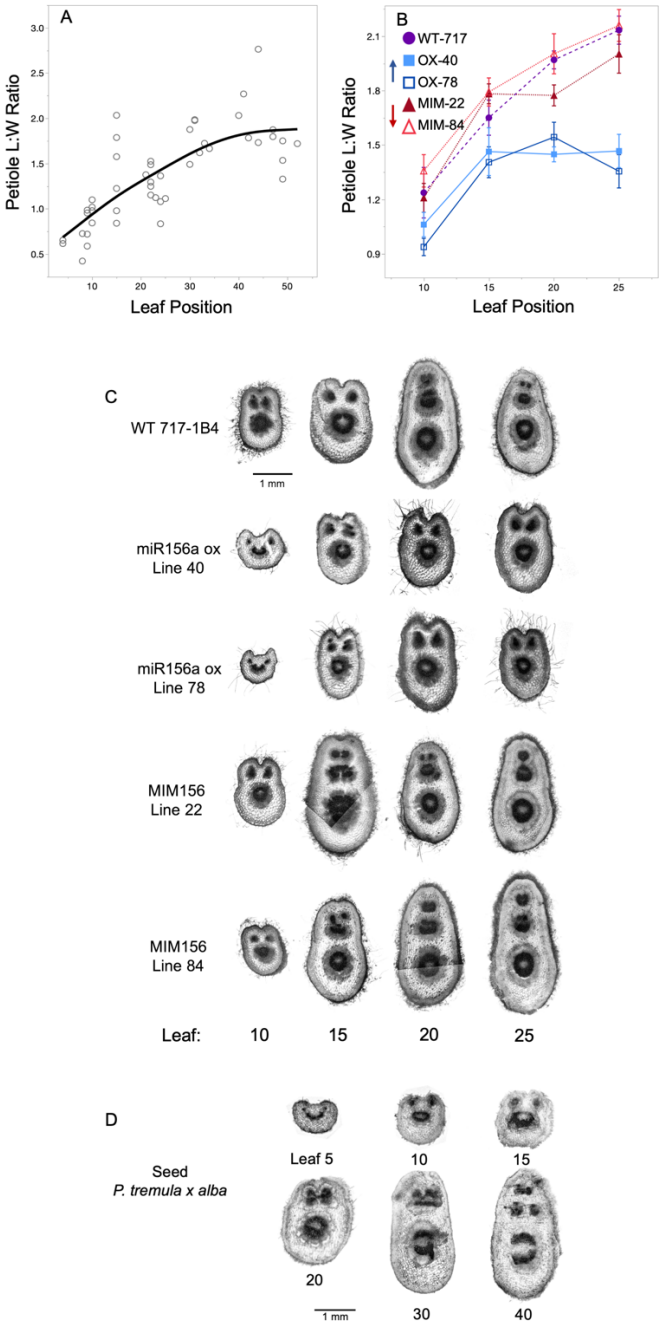

Figure 7. Petiole length:width ratio from cross sections made within 1 cm of leaf attachment in seed-grown (A) and 717-1B4 and transgenic poplar (B). Data from seed-grown plants presented as individual biological replicates using grey open circles and a mean best fit line in black or as means ± s.e.m with 717 wildtype data depicted by purple circles, miR156a overexpression lines depicted by blue squares and MIM156 lines depicted by red triangles (n = 7-12). Data from panel A show a second-degree polynomial relationship with p <0.0001 and R^2 = 0.62. For panel B, ANCOVA with leaf position and genotype as the effects found p< 0.0001 for leaf position and genotype and p=0.01 for the interaction. Representative samples of petiole cross sections from leaves 10, 15, 20 and 25 of the 717-1B4 and four transgenic lines (C). Representative samples of petiole cross sections from leaf positions between 5 and 40 in plants grown from seed (D).

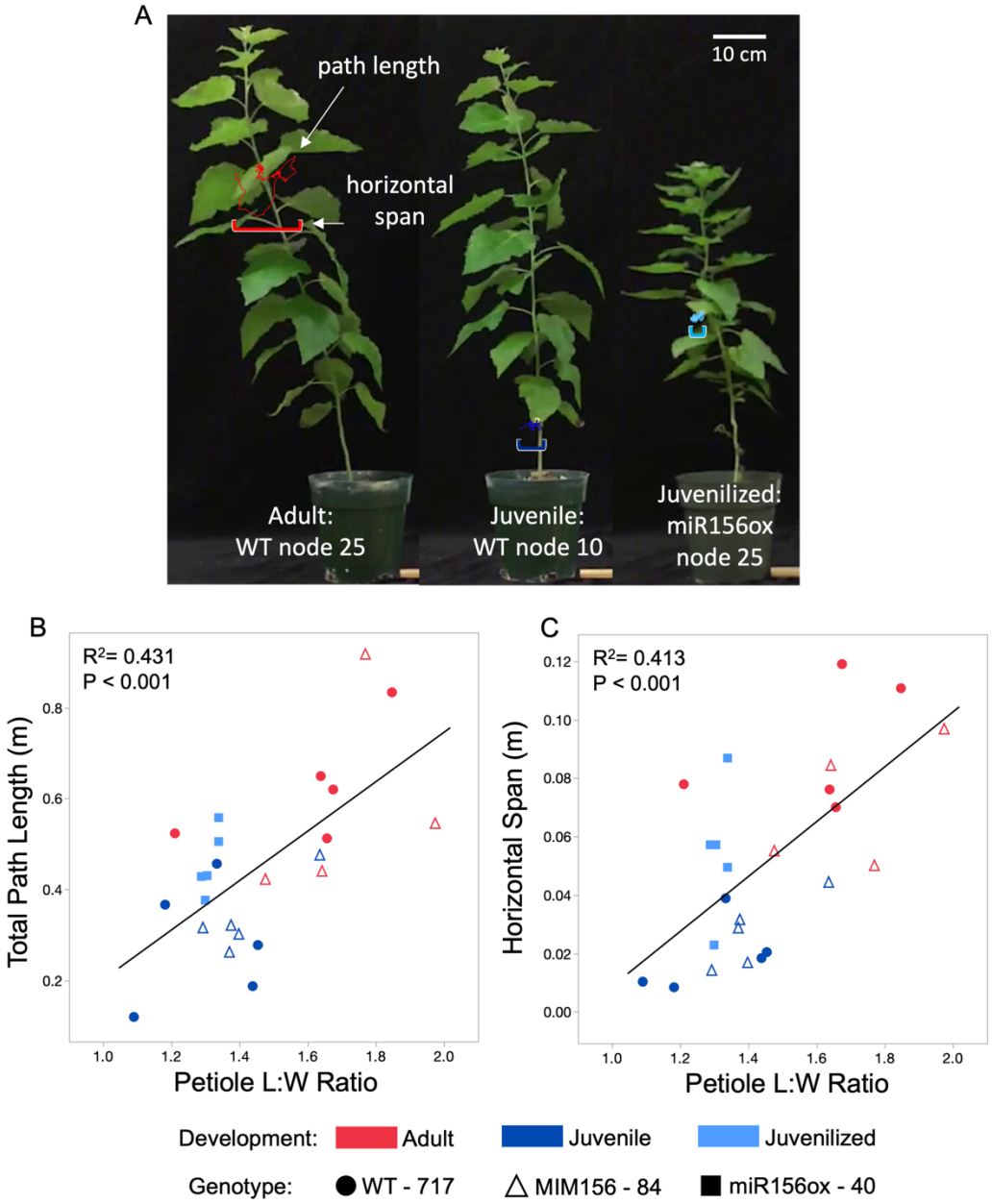

Figure 8. Diagram showing the path length and horizontal span measurements of leaf fluttering of an adult (WT 717-1B4 node 25), juvenile (WT 717-1B4 node 10), and juvenilized (miR156 overexpressor line 40 node 25) leaf. Quantification of leaf fluttering through total path length over a 1 second period (A) and maximum horizontal span of the tip of the leaf (B) and their relationship with petiole length:width ratio. 717-1B4 data is depicted by circles, miR156a ox line 40 by squares and MIM156 line 84 by triangles. Leaf developmental stage is noted by color with adult leaves in red, juvenile in dark blue and juvenilized in light blue. Linear fit for panel B) path length = -0.34288 + 0.544(petiole L:W ratio) and C) horizontal span = -0.0852 + 0.0939(petiole L:W ratio).